

Electronic Supplementary Information (ESI)

Neutron activation of In(III) complexes with thiosemicarbazones leads to the production of potential radiopharmaceuticals for the treatment of breast cancer

Alexandre A. Oliveira^a, Lucas L. Franco^a, Raquel G. dos Santos^b, Gabriele M. C. Perdigão^c, Jeferson G. da Silva^d, Elaine M. Souza-Fagundes^c, Heloisa Beraldo^{a,*}

^a Departamento de Química, Universidade Federal de Minas Gerais, 31270-901 Belo Horizonte, MG, Brazil.

^b Centro de Desenvolvimento da Tecnologia Nuclear, CDTN, 31270-901 Belo Horizonte, MG, Brazil.

^c Departamento de Fisiologia e Biofísica, Universidade Federal de Minas Gerais, 31270-901 Belo Horizonte, MG, Brazil.

^d Departamento de Farmácia, Universidade Federal de Juiz de Fora, Campus Governador Valadares, 35010-177 Governador Valadares, MG, Brazil.

*Corresponding author. Phone number: +55 (31) 3409-5740.

E-mail address: hberaldo@ufmg.br

heloisaberaldoufmg@gmail.com (H. Beraldo)

Table of contents

	Page
Spectroscopic characterization	2
Figure S1. Syntheses of the In(III) complexes with 2-acetylpyridine-derived thiosemicarbazones and carbon atom numbering. R = <i>o</i> Cl (1) or <i>p</i> F (2). Figure S2. ^1H NMR spectra of (a) ligand H2Ac4 <i>o</i> ClPh and (b) complex 1 (DMSO- d_6). Figure S3. $^{13}\text{C}\{\text{H}\}$ NMR and DEPT-135 spectra of (a) ligand H2Ac4 <i>o</i> ClPh and (b) complex 1 (DMSO- d_6). Figure S4. Contour map of 2D COSY experiment of the complex 1 (DMSO- d_6) exhibiting the homonuclear ^1H - ^1H correlations. Figure S5. Contour map of 2D HMQC experiment of the complex 1 (DMSO- d_6) exhibiting the most important heteronuclear ^1H - ^{13}C correlations. Figure S6. Contour map of 2D HMBC experiment of the complex 1 (DMSO- d_6) exhibiting the most important heteronuclear ^1H - ^{13}C correlations. Figure S7. FT-IR spectrum of ligand H2Ac4 <i>o</i> ClPh and complex 1 (KBr pellet). Figure S8. High Resolution Mass Spectra [ESI(+), IT-TOF] of 1 Figure S9. High Resolution Mass Spectra [ESI(+), IT-TOF] of 2	2 3 4 5 5 6 6 7 7
X-ray crystallography	8
Table S10. Bond lengths (Å) and angles (°) for 1a in comparison with the parent ligand	8
Cytotoxic activity	
Figure S11. Percentage of cell survival of MCF-7 cells vs drug concentration for (a) InCl ₃ and *InCl ₃ ; (b) In(NO ₃) ₃ and *In(NO ₃) ₃	9
Figure S12. Percentage of cell survival of MCF-7 cells vs drug concentration for (a) 1 and * 1 ; (b) 2 and * 2 ; (c) 3 and * 3 ; (d) 4 and * 4	10
Figure S13. Percentage of cell survival of MRC-5 cells vs drug concentration for (a) 1 and * 1 ; (b) 2 and * 2 ; (c) 3 and * 3 ; (d) 4 and * 4	11

Spectroscopic characterization

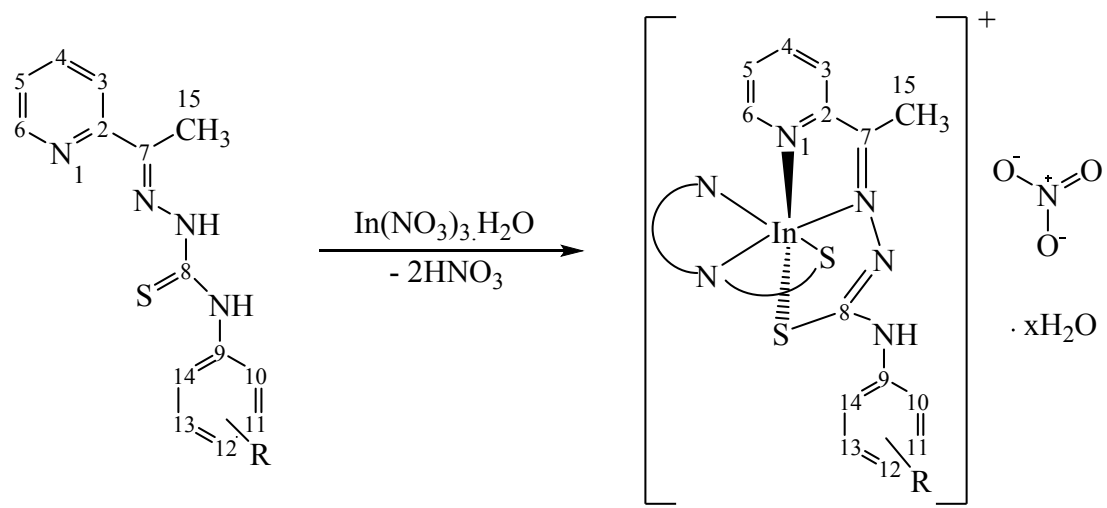


Figure S1. Syntheses of the In(III) complexes with 2-acetylpyridine-derived thiosemicarbazones and carbon atom numbering. R = *o*Cl (**1**) or *p*F (**2**).

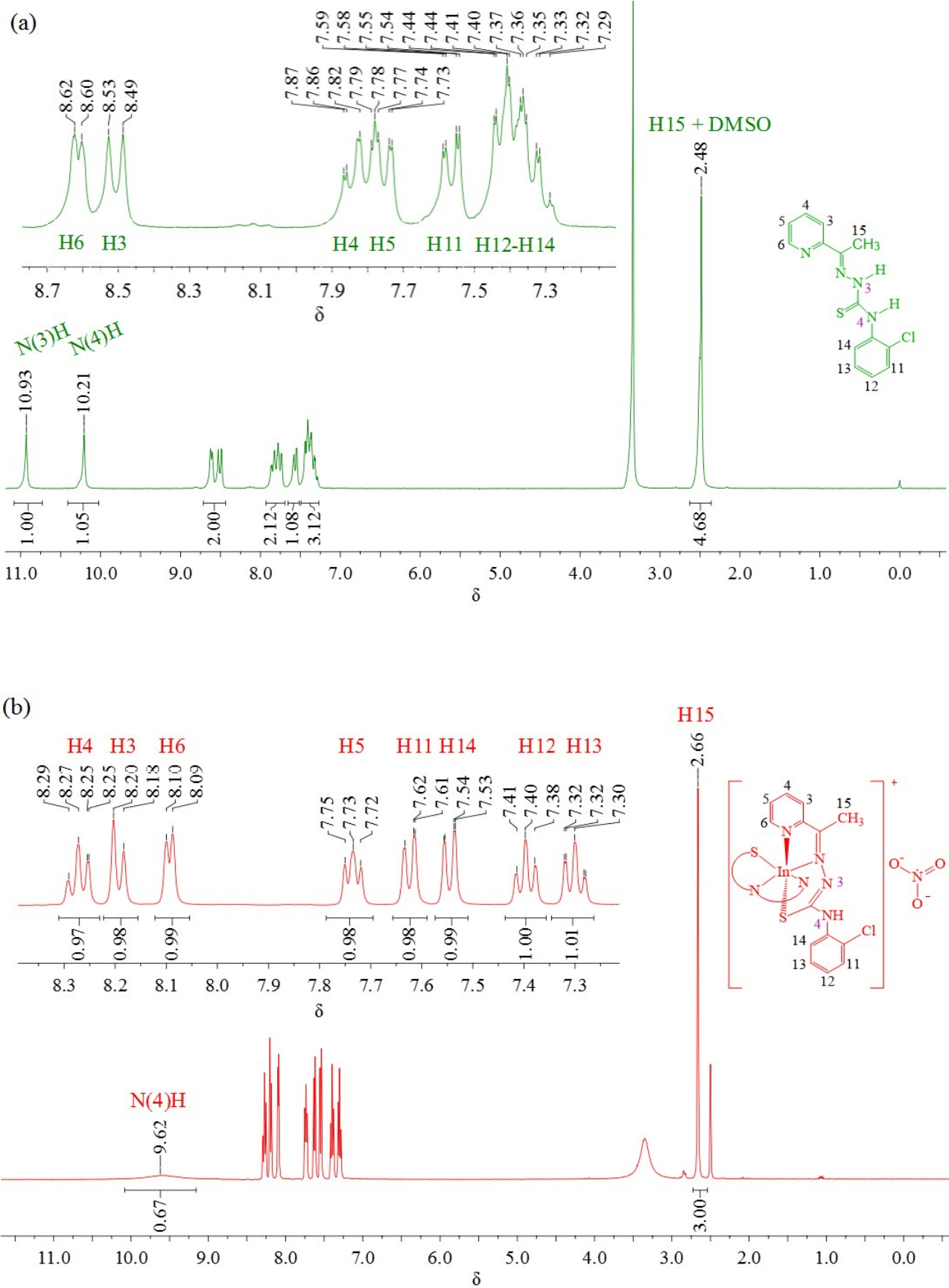
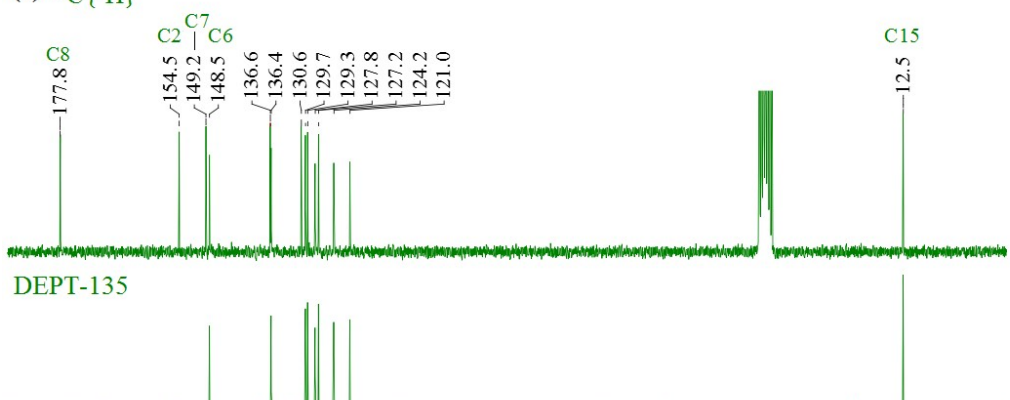


Figure S2. ^1H NMR spectra of (a) ligand H2Ac4oClPh and (b) complex **1** ($\text{DMSO}-d_6$).

(a) $^{13}\text{C}\{\text{H}\}$ 

(b)

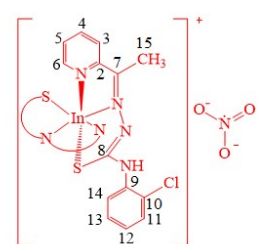
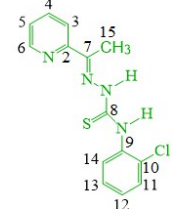
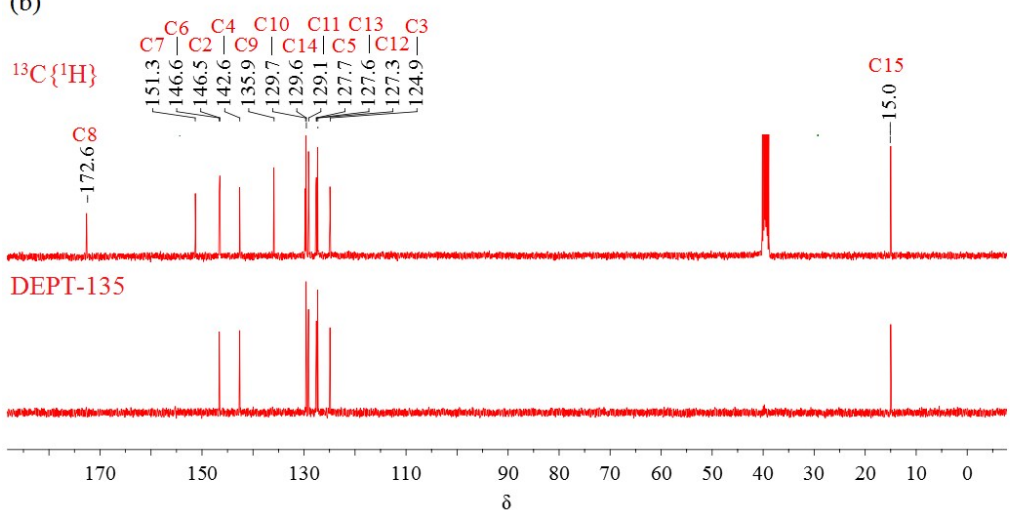


Figure S3. $^{13}\text{C}\{\text{H}\}$ NMR and DEPT-135 spectra of (a) ligand $\text{H}_2\text{Ac}4\text{oClPh}$ and (b) complex **1** ($\text{DMSO}-d_6$).

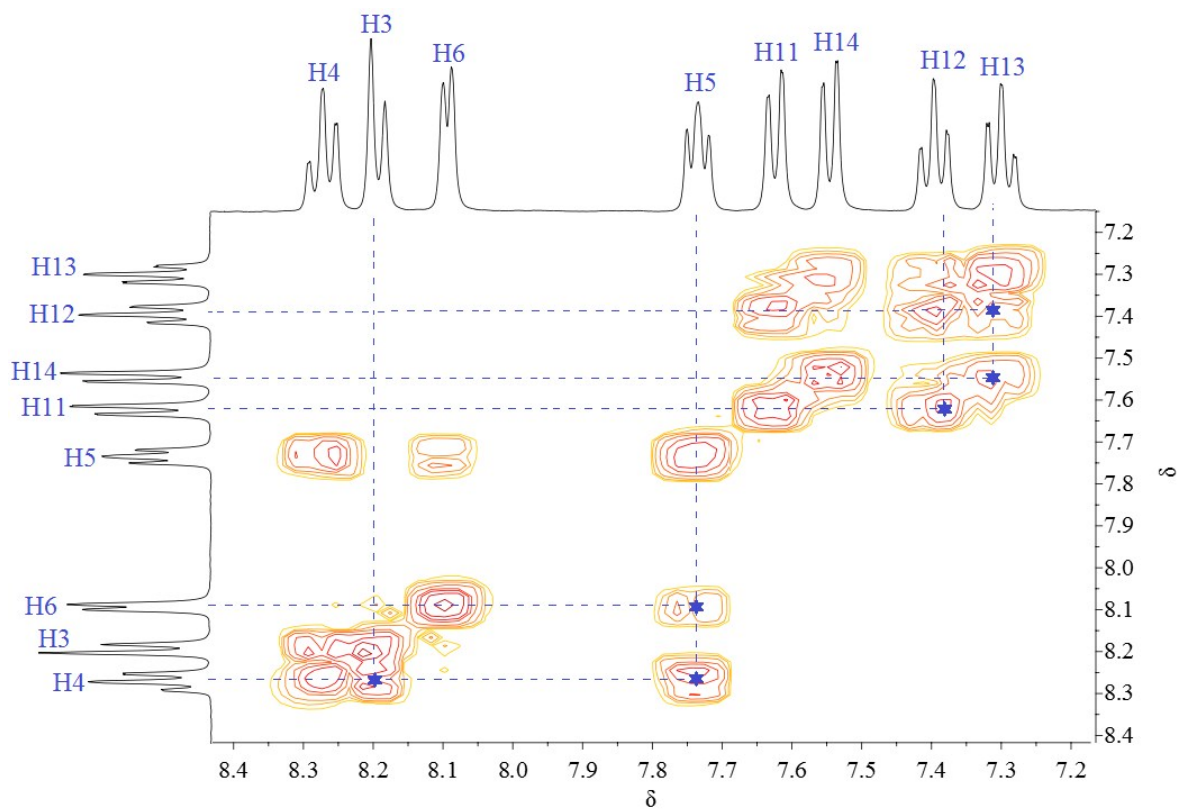


Figure S4. Contour map of 2D COSY experiment of the complex **1** ($\text{DMSO}-d_6$) exhibiting the homonuclear ^1H - ^1H correlations.

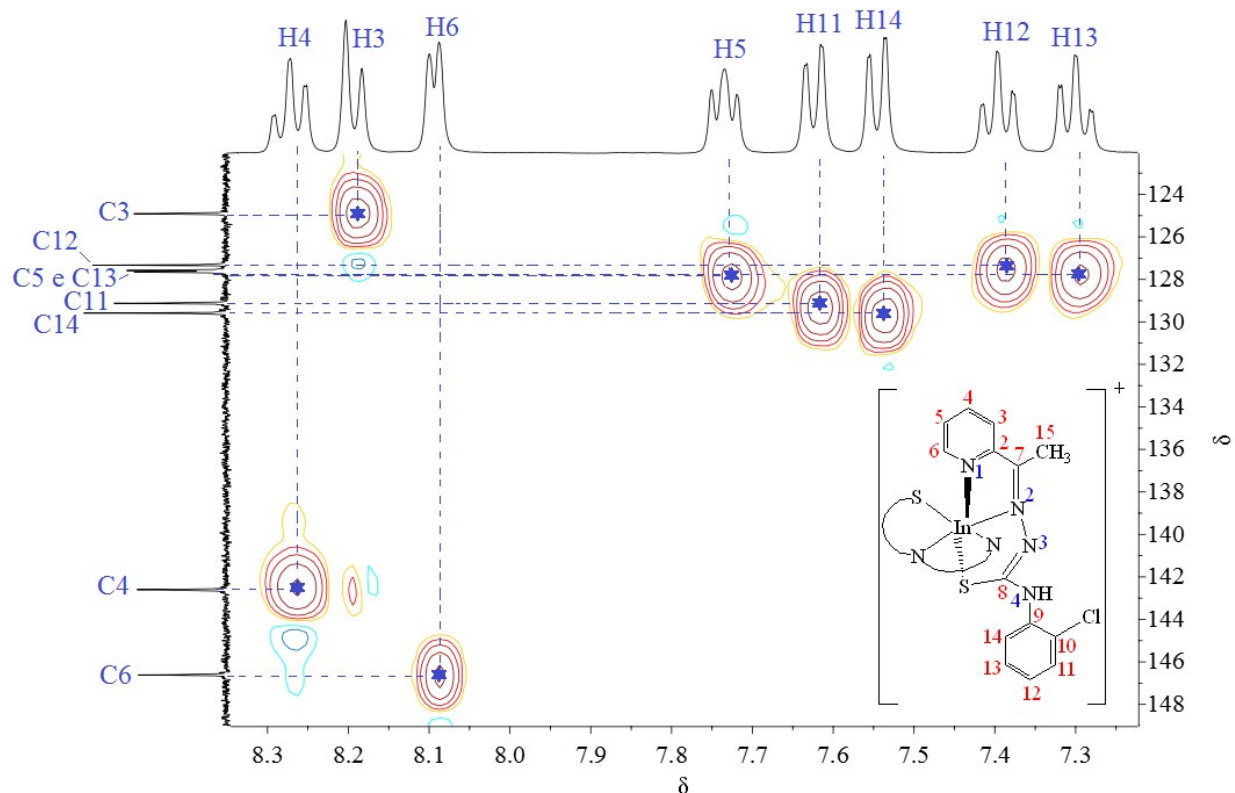


Figure S5. Contour map of 2D HMQC experiment of the complex **1** ($\text{DMSO}-d_6$) exhibiting the most important heteronuclear ^1H - ^{13}C correlations.

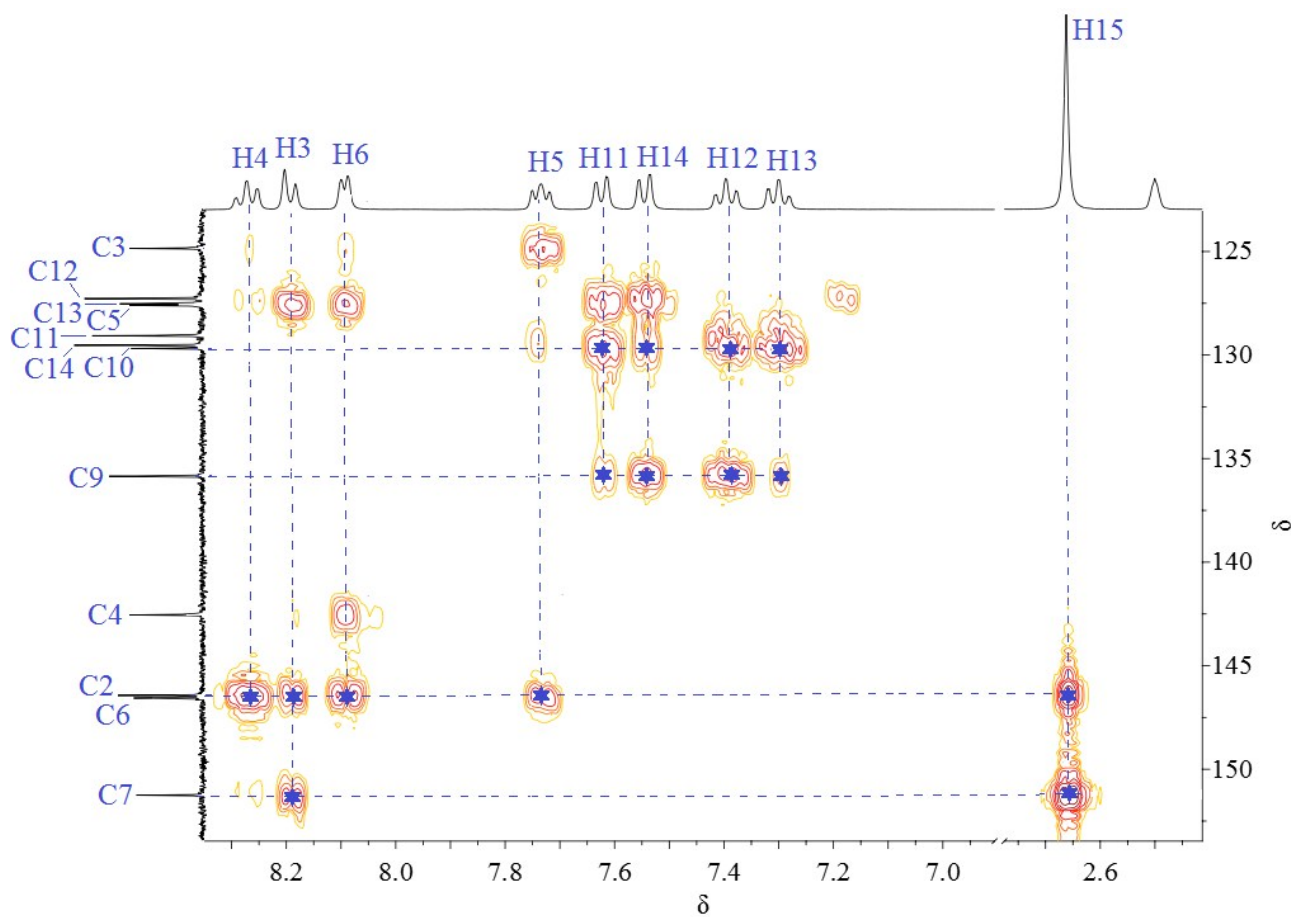


Figure S6. Contour map of 2D HMBC experiment of the complex **1** ($\text{DMSO}-d_6$) exhibiting the most important heteronuclear ^1H - ^{13}C correlations.

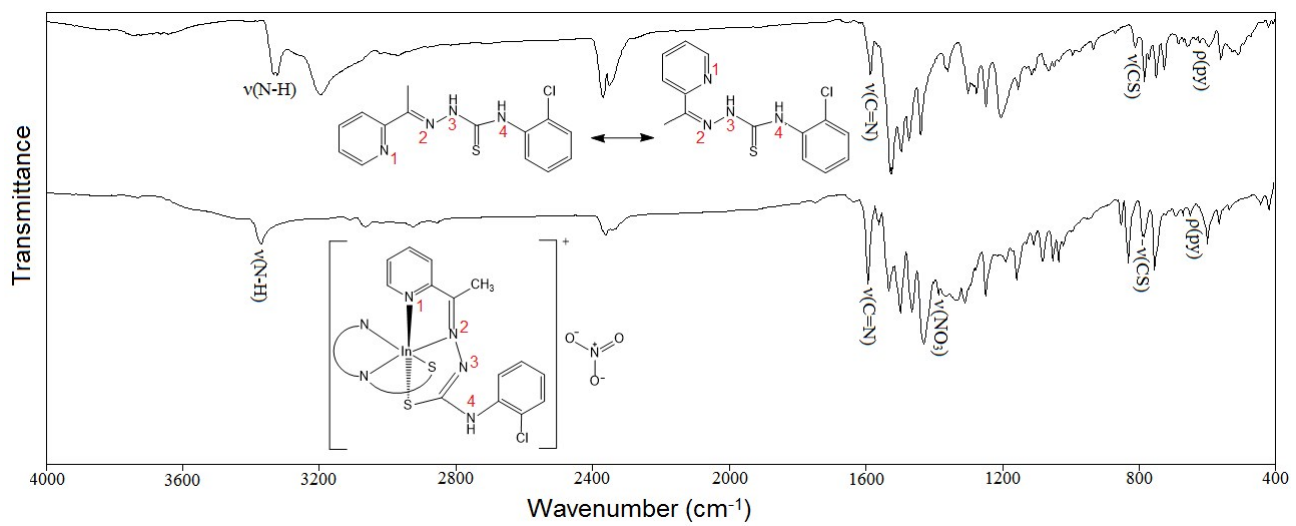


Figure S7. FT-IR spectrum of ligand $\text{H}_2\text{Ac}4\text{oClPh}$ and complex **1** (KBr pellet).

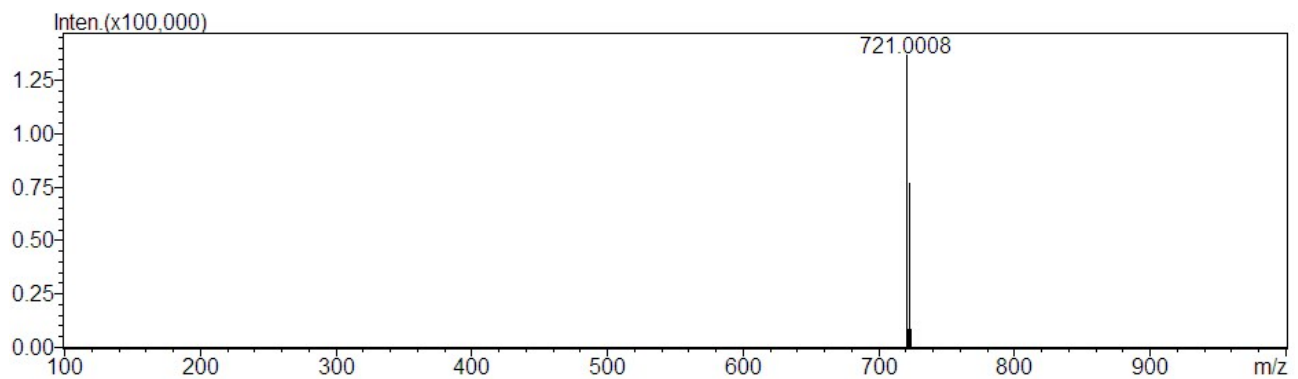


Figure S8. High Resolution Mass Spectra [ESI(+), IT-TOF] of **1**

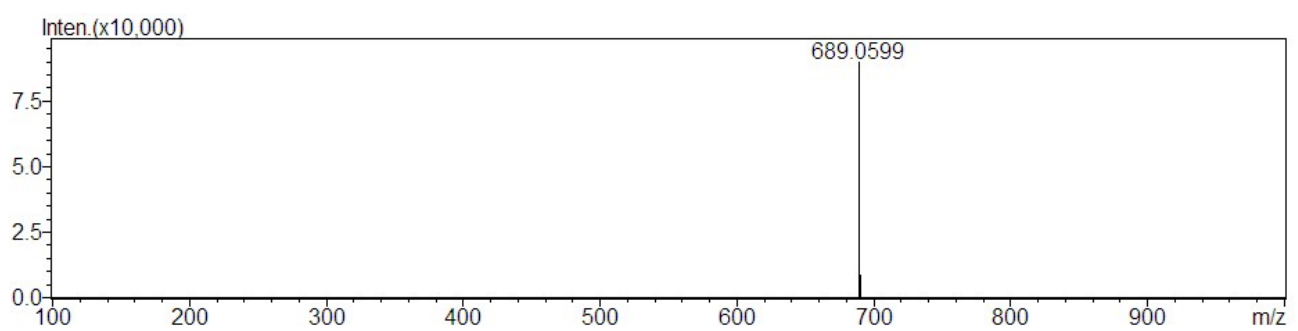


Figure S9. High Resolution Mass Spectra [ESI(+), IT-TOF] of **2**

X-ray crystallography

Table S10. Selected bond lengths (\AA) and angles ($^{\circ}$) for **1a** in comparison with the parent ligand¹

Bond	H2Ac4oClPh^a	1a^b
S1–C8	1.654(3)/1.654(3)	1.755(4)/1.756(4)
N2–C7	1.281(3)/1.278(3)	1.292(5)/1.292(4)
N2–N3	1.362(3)/1.361(3)	1.376(4)/1.381(4)
N3–C8	1.359(3)/1.351(3)	1.309(5)/1.315(5)
In1–N1	-	2.287(3)
In1–N2	-	2.264(3)
In1–S1	-	2.5028(10)
In1–N11	-	2.275(3)
In1–N12	-	2.264(3)
In1–S11	-	2.5018(10)
C7–N2–N3	119.1(2)/118.7(2)	117.6(3)/117.7(3)
N2–N3–C8	118.2(2)/118.9(2)	114.1(3)/114.7(3)
N3–C8–S1	121.0(2)/121.5(2)	128.9(3)/128.5(3)
N1–In1–N2	-	71.01(11)
N1–In1–S1	-	145.75(8)
N1–In1–N11	-	84.77(11)
N1–In1–N12	-	97.24(10)
N1–In1–S11	-	97.12(8)
N2–In1–S1	-	77.04(8)
N2–In1–N11	-	106.74(11)
N2–In1–N12	-	168.25(11)
N2–In1–S11	-	103.42(8)
S1–In1–N11	-	93.03(8)
S1–In1–N12	-	114.40(8)
S1–In1–S11	-	102.02(4)
N11–In1–N12	-	71.30(10)
N11–In1–S11	-	148.62(8)
N12–In1–S11	-	77.41(8)

^a The two values of bond distances and angles in H2Ac4oClPh refer to the two molecules in the asymmetric unit. ^b For **1a** the two values refer to the two ligands coordinated to the metal center.

¹ J. A. Lessa, I. C. Mendes, P. R. O. Silva, M. A. Soares, R. G. Santos, N. L. Speziali, N. C. Romeiro, E. J. Barreiro, H. Beraldo, *Eur. J. Med. Chem.*, 2010, **45**(12), 5671-5677.

Cytotoxic activity

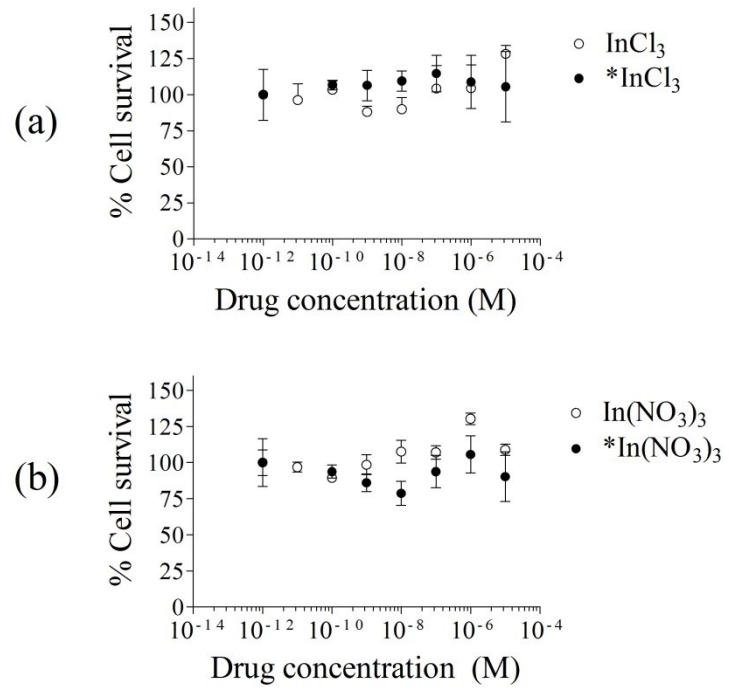


Figure S11. Percentage of cell survival of MCF-7 cells *vs* drug concentration for (a) InCl₃ and *InCl₃; (b) In(NO₃)₃ and *In(NO₃)₃

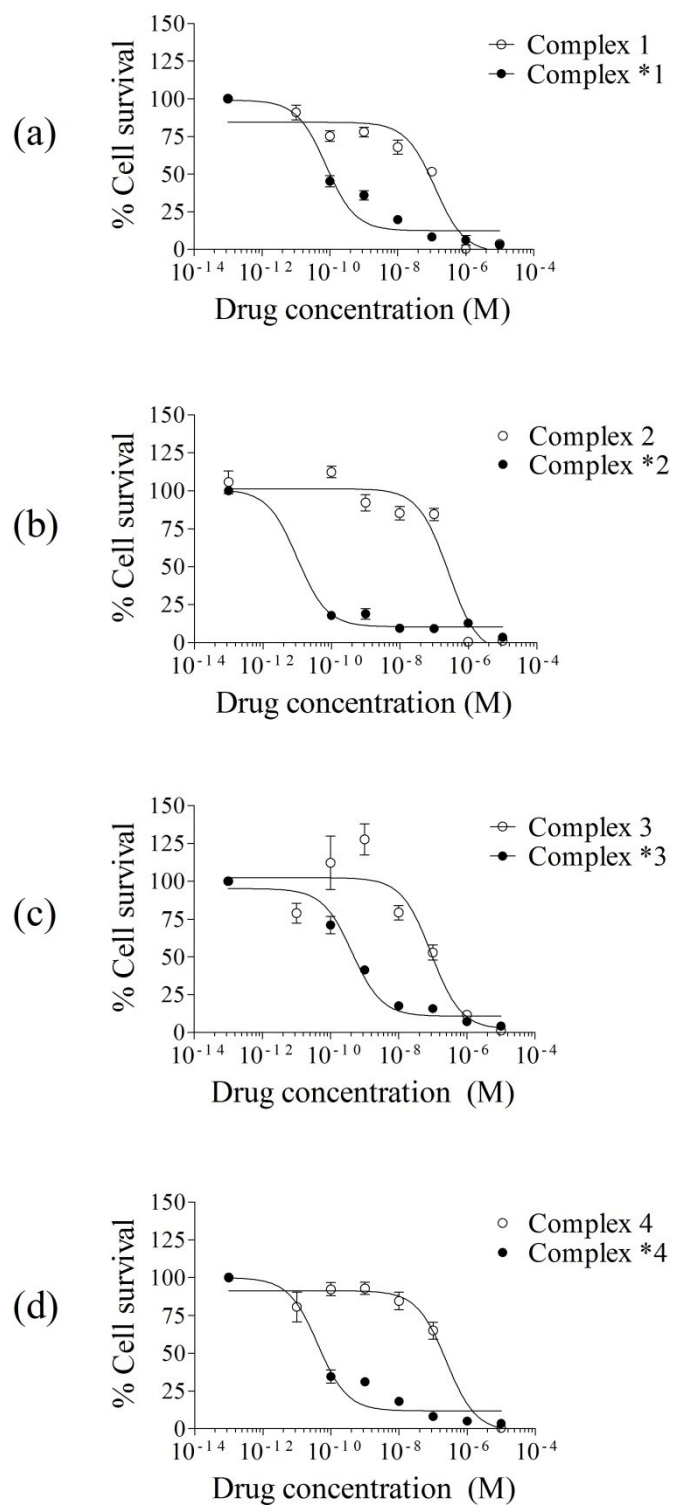


Figure S12. Percentage of cell survival of MCF-7 cells *vs* drug concentration for (a) **1** and ***1**; (b) **2** and ***2**; (c) **3** and ***3**; (d) **4** and ***4**.

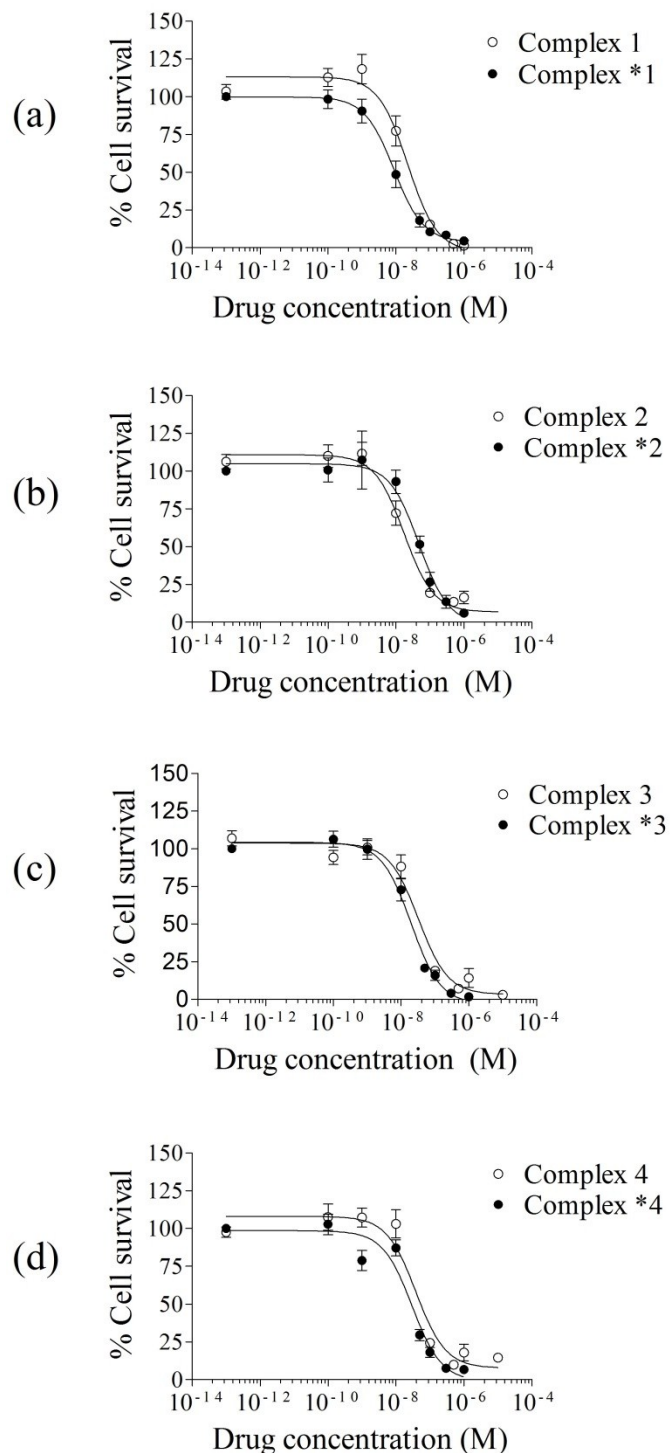


Figure S13. Percentage of cell survival of MRC-5 cells *vs* drug concentration for (a) **1** and ***1**; (b) **2** and ***2**; (c) **3** and ***3**; (d) **4** and ***4**.